Available online at www.sciencedirect.com
SCIENCE DIRECT®
Optics Communications 246 (2005) 241–248
OPTICS COMMUNICATIONS
www.elsevier.com/locate/optcom

Comparison between complex amplitude envelope representation and complex analytic signal representation in studying pulsed Gaussian beam

Runwu Peng *, Dianyuan Fan

Shanghai Institute of Optics and Fine Mechanics, Chinese Academy of Sciences, P.O. Box 800-211, Shanghai 201800, China

Received 8 April 2004; received in revised form 27 October 2004; accepted 2 November 2004

Abstract

Analytic propagation expressions of pulsed Gaussian beam are deduced by using complex amplitude envelope representation and complex analytic signal representation. Numerical calculations are given to illustrate the differences between them. The results show that the major difference between them is that there exists singularity in the beam obtained by using complex amplitude envelope representation. It is also found that singularity presents near propagation axis in the case of broadband and locates far from propagation axis in the case of narrowband. The critical condition to determine what representation should be adopted in studying pulsed Gaussian beam is also given.

PACS: 42.25.Bs; 42.25.Fx; 42.60.Jf
Keywords: Complex amplitude envelope; Complex analytic signal; Narrowband pulsed beam; Broadband pulsed beam

1. Introduction

Propagation properties of pulsed laser beams have been studied in several works in recent years [1–9]. In some of these works, complex amplitude envelope (CAE) representation has been introduced when slowly varying envelope approximation (SVEA) is performed, from which simplified expressions can be obtained. The condition that SVEA theory can be performed, however, is $\Delta\omega/\omega_0 \ll 1$, where $\Delta\omega$ is FWHM (full width at half maximum) spectral width of the pulse and ω_0 is the carrier frequency. For ultrashort pulsed laser beam, which already has broad spectra, the condition $\Delta\omega/\omega_0 \ll 1$ is not satisfied any more. If the SVEA theory is still performed to study the propagation properties of such pulsed beam with broadband, the pulsed beam obtained by using CAE

* Corresponding author. Tel.: +86 21 6991 8810.
E-mail addresses: pengrunwu@siom.ac.cn, pengrunwu@sina.com (R. Peng).

0030-4018/$ - see front matter © 2004 Elsevier B.V. All rights reserved.
doi:10.1016/j.optcom.2004.11.006

representation will present "anti-beam" behavior [2,4], i.e., singularity emerges, which loses physical meaning. In order to avoid this phenomenon, rigorous complex analytic signal (CAS) [10] should be adopted [4]. However, to what value of $\Delta\omega/\omega_0$ is CAE representation applicable? This is an interesting question in the study of pulsed Gaussian beam (PGB). Another interesting question is how differences between the PGB obtained by using CAE representation (CAE solution for short) and that obtained by using CAS representation (CAS solution for short) for a fixed value of $\Delta\omega/\omega_0$.

In the present paper we investigate the propagation properties of the PGB with different bandwidth in free space and discuss the above questions during the study. Propagation expressions of CAE solution and CAS solution of pulsed beams are deduced in Section 2. Taking the PGB as an example, propagation expressions of CAE solution and CAS solution of the beam are given in Section 3. Comparisons between them are made by numerical calculations in Section 4. Finally, in Section 5 the main results obtained in this paper are summarized.

2. Propagation expressions of pulsed beam in free space

It is well known that the scalar wave equation in frequency-domain is given by

$$(\nabla^2 + k^2)V(r,z,\omega) = 0, \tag{1}$$

where $\nabla^2 = \partial^2/\partial x^2 + \partial^2/\partial y^2 + \partial^2/\partial z^2$ is the Laplacian operator, $r^2 = x^2 + y^2$, $k = \omega/c$ is wave number and V the complex scalar field. By introducing $V(r,z,\omega) = V_0(r,z,\omega)\exp(-ikz)$, where V_0 is field amplitude, and performing the paraxial approximation, Eq. (1) can be written as

$$\left(\nabla_\perp^2 - 2ik\frac{\partial}{\partial z}\right)V_0(r,z,\omega) = 0, \tag{2}$$

where $\nabla_\perp^2 = \partial^2/\partial x^2 + \partial^2/\partial y^2$ is the transversal Laplacian operator. A fundamental solution of Eq. (2) is given by [11]

$$V_0(r,z,\omega) = \frac{iz_R}{z+iz_R}\exp\left(-i\frac{kr^2}{2(z+iz_R)}\right)P(\omega), \tag{3}$$

where z_R denotes the Rayleigh diffraction length and $P(\omega)$, a parameter only related to frequency, is field at $r = 0$ and $z = 0$ in the frequency-space. The temporal-domain pulsed field can be derived from the inverse Fourier transform of Eq. (3)

$$V(r,z,t) = \frac{1}{\sqrt{2\pi}}\int_{-\infty}^{\infty}\frac{iz_R}{z+iz_R}P(\omega) \times \exp\left\{i\omega\left[t - \frac{z}{c} - \frac{r^2}{2c(z+iz_R)}\right]\right\}d\omega. \tag{4}$$

Because $z_R = kw_0^2/2$ is independent of frequency for isodiffracting pulsed beam, where w_0 is waist width, analytic solution is obtained as

$$V(r,z,t) = \frac{iz_R}{z+iz_R}P(\tau), \tag{5}$$

where

$$P(\tau) = \frac{1}{\sqrt{2\pi}}\int_{-\infty}^{\infty}P(\omega)\exp(i\omega\tau)\,d\omega, \tag{6}$$

$$\tau = t - \frac{z}{c} - \frac{r^2}{2c(z+iz_R)}. \tag{7}$$

Consider a real pulse at $r = 0$ and $z = 0$ of the form

$$p(t) = A(t)\cos(\omega_0 t + \varphi), \tag{8}$$

where $A(t) \geqslant 0$ is the pulse envelope and φ its associated phase factor. Fourier spectrum of $p(t)$ is given by

$$P(\omega) = \frac{1}{\sqrt{2\pi}}\int_{-\infty}^{\infty}p(t)\exp(-i\omega t)\,dt = \frac{1}{2}[g(\omega-\omega_0) + g^*(-\omega-\omega_0)], \tag{9}$$

where

$$g(\omega) = \frac{1}{\sqrt{2\pi}}\int_{-\infty}^{\infty}A(t)\exp(-i\varphi)\exp(-i\omega t)\,dt. \tag{10}$$

The complex field $P(t)$ of the real pulse $p(t)$ [$\mathrm{Re}P(t) = p(t)$] in Eq. (8) is obtained by substituting t for τ in Eq. (6). $P(t)$ should be represented as rigorous complex analytic signal, namely

$$P_{\mathrm{CAS}}(t)=\frac{2}{\sqrt{2\pi}}\int_0^{\infty}P(\omega)\exp(\mathrm{i}\omega t)\,\mathrm{d}\omega. \tag{11}$$

Thus, substituting from Eq. (9) into Eq. (11), it is obtained

$$P_{\mathrm{CAS}}(t)=\frac{1}{\sqrt{2\pi}}\int_0^{\infty}[g(\omega-\omega_0)+g^*(-\omega-\omega_0)]\times\exp(\mathrm{i}\omega t)\,\mathrm{d}\omega. \tag{12}$$

For pulsed beam with narrowband ($\Delta\omega/\omega_0\ll 1$), $g(\omega-\omega_0)$ takes appreciable values only within small interval. In such case the term $g^*(-\omega-\omega_0)$ can be neglected and the lower integration limit can be extended to $-\infty$ [4]. Therefore, Eq. (12) can be written as follows:

$$P_{\mathrm{CAE}}(t)=\frac{1}{\sqrt{2\pi}}\int_{-\infty}^{\infty}g(\omega-\omega_0)\exp(\mathrm{i}\omega t)\,\mathrm{d}\omega=A(t)\exp(\mathrm{i}\varphi)\exp(\mathrm{i}\omega_0 t), \tag{13}$$

$A(t)\exp(\mathrm{i}\varphi)$ is complex amplitude envelope and Eq. (13) is CAE representation, which is approximation of CAS representation in the case of narrowband ($\Delta\omega/\omega_0\ll 1$). Hence, $P(\tau)$ can be expressed by using CAE representation Eq. (13) when the SVEA theory is performed. Substituting from Eq. (13) into Eq. (5) yields

$$V_{\mathrm{CAE}}(r,z,t)=\frac{\mathrm{i}z_{\mathrm{R}}}{z+\mathrm{i}z_{\mathrm{R}}}A(\tau)\exp[\mathrm{i}(\omega_0\tau+\varphi)]. \tag{14}$$

For pulsed beam with broadband, however, there is $\Delta\omega/\omega_0\sim 1$ and SVEA theory could not be performed. Therefore, $P(\tau)$ should be expressed by using CAS representation Eq. (12) rather than CAE representation Eq. (13). Substituting from Eq. (12) into Eq. (5), the pulsed beam with broadband is obtained of the form

$$V_{\mathrm{CAS}}(r,z,t)=\frac{\mathrm{i}z_{\mathrm{R}}}{z+\mathrm{i}z_{\mathrm{R}}}\frac{1}{\sqrt{2\pi}}\int_0^{\infty}[g(\omega-\omega_0)+g^*(-\omega-\omega_0)]\exp(\mathrm{i}\omega\tau)\,\mathrm{d}\omega. \tag{15}$$

3. Examples

Consider a PGB whose real form at $r=z=0$ is given by

$$p(t)=\exp\left[-\left(a_{\mathrm{g}}\frac{t}{T}\right)^2\right]\cos(\omega_0 t+\varphi), \tag{16}$$

where $a_{\mathrm{g}}=\sqrt{2\ln 2}$ and T is pulse duration (FWHM). From Eq. (9), Fourier spectrum of the PGB is obtained as

$$P(\omega)=\frac{T}{\sqrt{2}a_{\mathrm{g}}}\exp\left(-\frac{T^2(\omega-\omega_0)^2}{2a_{\mathrm{g}}^2}\right). \tag{17}$$

Substituting from Eq. (17) into Eq. (11), CAS representation of the PGB is deduced as

$$P_{\mathrm{CAS}}(t)=\frac{1}{2}\exp\left(-a_{\mathrm{g}}^2\frac{t^2}{T^2}\right)\left\{\exp(-\mathrm{i}\omega_0 t-\mathrm{i}\varphi)\times\left[1-\mathrm{erf}\left(\frac{T\omega_0}{2a_{\mathrm{g}}}-\mathrm{i}a_{\mathrm{g}}\frac{t}{T}\right)\right]+\exp(\mathrm{i}\omega_0 t+\mathrm{i}\varphi)\times\left[1-\mathrm{erf}\left(-\frac{T\omega_0}{2a_{\mathrm{g}}}-\mathrm{i}a_{\mathrm{g}}\frac{t}{T}\right)\right]\right\}, \tag{18}$$

where erf( ) is the error function. For the PGB with narrowband ($\Delta\omega/\omega_0\ll 1$), Eq. (18) can be expressed by using CAE representation

$$P_{\mathrm{CAE}}(t)=\exp\left[-\left(a_{\mathrm{g}}\frac{t}{T}\right)^2\right]\exp(\mathrm{i}\omega_0 t+\mathrm{i}\varphi). \tag{19}$$

Substituting from Eq. (19) into Eq. (5), CAE solution of the PGB with narrowband is obtained as

$$V_{\mathrm{CAE}}(r,z,t)=\frac{\mathrm{i}z_{\mathrm{R}}}{z+\mathrm{i}z_{\mathrm{R}}}\times\exp\left[\mathrm{i}(\omega_0\tau+\varphi)-(a_{\mathrm{g}}\gamma\omega_0\tau)^2\right], \tag{20}$$

where $\gamma=\Delta\omega/\omega_0=1/\omega_0 T$ denotes bandwidth. Substituting from Eq. (18) into Eq. (5), CAS solution of the PGB with broadband ($\Delta\omega/\omega_0\sim 1$) is given by

$$V_{\mathrm{CAS}}(r,z,t)=\frac{\mathrm{i}z_{\mathrm{R}}}{2(z+\mathrm{i}z_{\mathrm{R}})}\exp\left[-(a_{\mathrm{g}}\gamma\omega_0\tau)^2\right]\times\left\{\exp(-\mathrm{i}\omega_0\tau-\mathrm{i}\varphi)\left[1-\mathrm{erf}\left(\frac{1}{2a_{\mathrm{g}}\gamma}-\mathrm{i}a_{\mathrm{g}}\gamma\omega_0\tau\right)\right]+\exp(\mathrm{i}\omega_0\tau+\mathrm{i}\varphi)\left[1-\mathrm{erf}\left(-\frac{1}{2a_{\mathrm{g}}\gamma}-\mathrm{i}a_{\mathrm{g}}\gamma\omega_0\tau\right)\right]\right\}. \tag{21}$$

4. Numerical calculations and analyses

Eqs. (20) and (21) are bases of numerical calculations and analyses in this paper. Firstly, we make a comparison between them in the form. Eq. (21) can be rewritten as

$$V_{\mathrm{CAS}}(r,z,t) = \frac{\mathrm{i}z_{\mathrm{R}}}{z+\mathrm{i}z_{\mathrm{R}}} \times \exp\left[\mathrm{i}(\omega_0\tau+\varphi) - (a_{\mathrm{g}}\gamma\omega_0\tau)^2\right]\xi, \tag{22}$$

where

$$\xi = \frac{1}{2}\left\{\exp[-2\mathrm{i}(\omega_0\tau+\varphi)]\left[1-\mathrm{erf}\left(\frac{1}{2a_{\mathrm{g}}\gamma} - \mathrm{i}a_{\mathrm{g}}\gamma\omega_0\tau\right)\right] + \left[1-\mathrm{erf}\left(-\frac{1}{2a_{\mathrm{g}}\gamma} - \mathrm{i}a_{\mathrm{g}}\gamma\omega_0\tau\right)\right]\right\}. \tag{23}$$

Compared with $V_{\mathrm{CAE}}(r,z,t)$, $V_{\mathrm{CAS}}(r,z,t)$ includes the term ξ, which is the main difference between CAE and CAS solutions. The lack of the term ξ in Eq. (20) is caused by neglected the term $g^*(-\omega-\omega_0)$ when CAE solution is deduced from Eq. (12) to Eq. (13). By using numerical calculations, the two solutions are compared detailedly as follows. Fig. 1 gives the radial and temporal waveforms of the PGB with $\gamma = 0.32$ ($T = 1.77$ fs) at $z = 3z_{\mathrm{R}} = 8.86\times10^3$ mm, where the calculation parameters are $w_0 = 1$ mm, $\lambda_0 = 1064$ nm ($\omega_0 = 1.77$ fs^{-1}, $T_0 = 3.55$ fs). As can be seen, differences between $I_{\mathrm{CAE}}(r,z,t) = |V_{\mathrm{CAE}}(r,z,t)|^2$ and $I_{\mathrm{CAS}}(r,z,t) = |V_{\mathrm{CAS}}(r,z,t)|^2$ become great with increasing radius r and singularity of $I_{\mathrm{CAE}}(r,z,t)$ emerges in the end. Obviously, the lack of ξ in $V_{\mathrm{CAE}}(r,z,t)$ results in the emergence of singularity of $I_{\mathrm{CAE}}(r,z,t)$ near z-axis ($r = 0$) for the PGB with broadband. The radial and temporal waveforms of the PGB with $\gamma = 0.08$ ($T = 7.1$ fs) at $z = 10z_{\mathrm{R}} = 2.95\times10^4$ mm are depicted in Fig. 2, where the calculation parameters are the same as those in Fig. 1. We can see that distributions of $I_{\mathrm{CAE}}(r,z,t)$ and $I_{\mathrm{CAS}}(r,z,t)$ are the same within the plotted region in Fig. 2. It is concluded from Figs. 1 and 2 that differences between CAE solution and CAS solution of the PGB are great in the case of broadband and few in the case of narrowband.

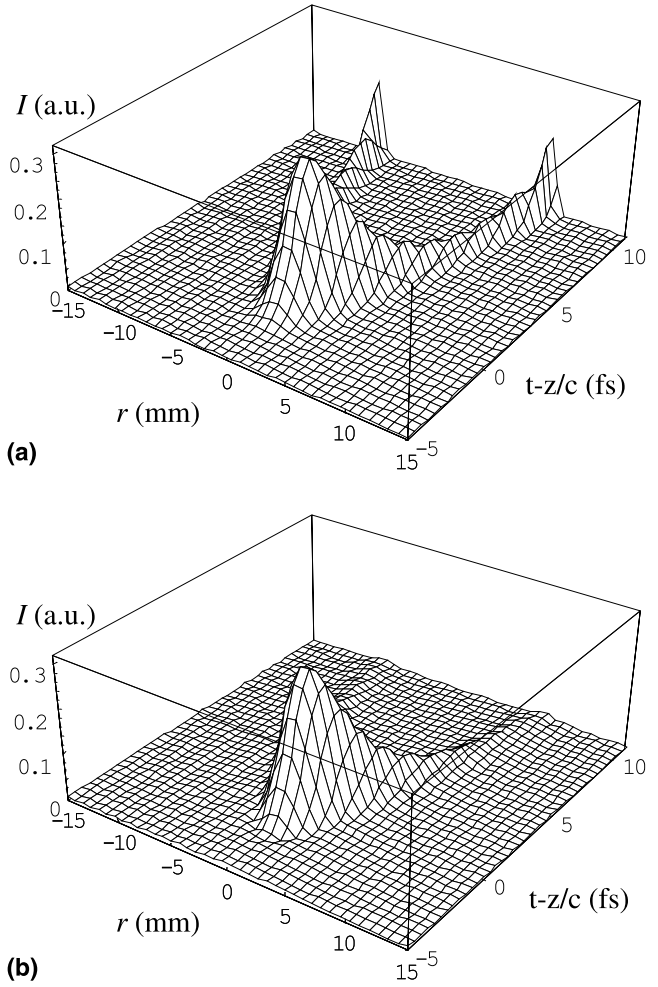

Fig. 1. Radial and temporal waveforms of the PGB with $\gamma = 0.32$ at $z = 3z_{\mathrm{R}} = 8.86\times10^3$ mm: (a) CAE solution; (b) CAS solution.

For the PGB with narrowband, however, there still exists singularity by using CAE representation, which can be seen from Fig. 3. The singularities' radial positions r_{s} of CAE solution of the PGB as a function of bandwidth is given in the figure, in which it is shown that the broader the pulse bandwidth, the nearer singularity locates to z-axis ($r = 0$), and vice versa. It is also seen that r_{s} of CAE solution of the PGB with $\gamma = 0.08$ at $z = 0$, z_{R} and $3z_{\mathrm{R}}$ are 11, 16 and 34 mm, and they are 3, 4 and 9 mm with $\gamma = 0.32$, respectively. If $r_{\mathrm{s}} > 10w_0$ is regarded as condition that the singularity can be neglected, CAE solution and CAS solution of the PGB are the same at $z = 0$ when bandwidth of the pulse is $\gamma = 0.08$. For the PGB with narrower

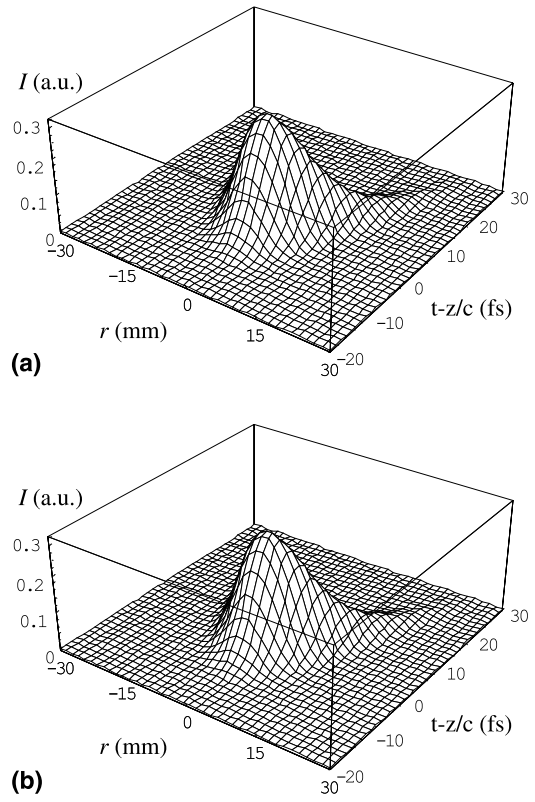

Fig. 2. Radial and temporal waveforms of the PGB with $\gamma = 0.08$ at $z = 10z_R = 2.95 \times 10^4$ mm: (a) CAE solution; (b) CAS solution.

bandwidth $\gamma = 0.01$ ($T = 56.5$ fs), the radial positions r_s of singularities are 85, 121 and 268 mm at $z = 0$, z_R and $3z_R$, respectively, which are

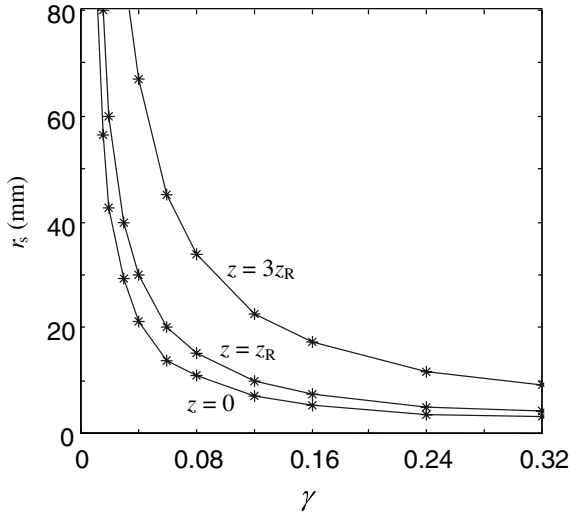

Fig. 3. Radial position r_s of singularity versus pulse bandwidth γ.

great distances that lead singularities have few effects on the study of pulse as compared with $w_0 = 1$ mm. Therefore, the approach in [2] is applicable to the PGB with narrowband.

It is also shown that there exists time delay of the peaks of off-axis pulse in comparison with that of the on-axis pulse in Figs. 1 and 2. According to Eq. (7), the complex time delay is given by

$$t' = \frac{r^2}{2c(z + \mathrm{i}z_R)}. \tag{24}$$

From Eq. (24), it is known that the farther the point locates from the z-axis, the more time delay there is.

The differences between CAE solution and CAS solution of the PGB can also be seen from the complex field distributions of them. Temporal waveforms of complex field of the PGB with $\gamma = 0.32$ are depicted in Fig. 4, which shows that differences between the real parts of V_{CAS} (solid lines) and that of V_{CAE} (dashed lines) are very small on the axis but great off the axis. From Fig. 4, it is also seen that V_{CAS} presents spatio-temporal couplings such as time delay of the peaks of off-axis field and frequency lessening with increasing r, whereas V_{CAE} only presents the time delay and is failed to show frequency shift. The time delay of both of them is given by Eq. (24). Fig. 5 gives temporal waveforms of complex field of the PGB with $\gamma = 0.08$, from which it is seen that the real parts of V_{CAS} (solid lines) and that of V_{CAE} (dashed lines) are the same and the lines coincide with each other both on and off the axis. In Fig. 5, both V_{CAS} and V_{CAE} present time delay and frequency shift. The calculation parameters of Figs. 4 and 5 are the same as those in Fig. 1. From the two figures, it is further concluded that CAE representation could only be used for the PGB with narrowband and rigorous CAS representation should be used in the case of broadband.

In order to explain the emergence of singularity and the effects of bandwidth on its radial position explicitly, Eq. (20) at $z = 0$ and $t = 0$ is written as

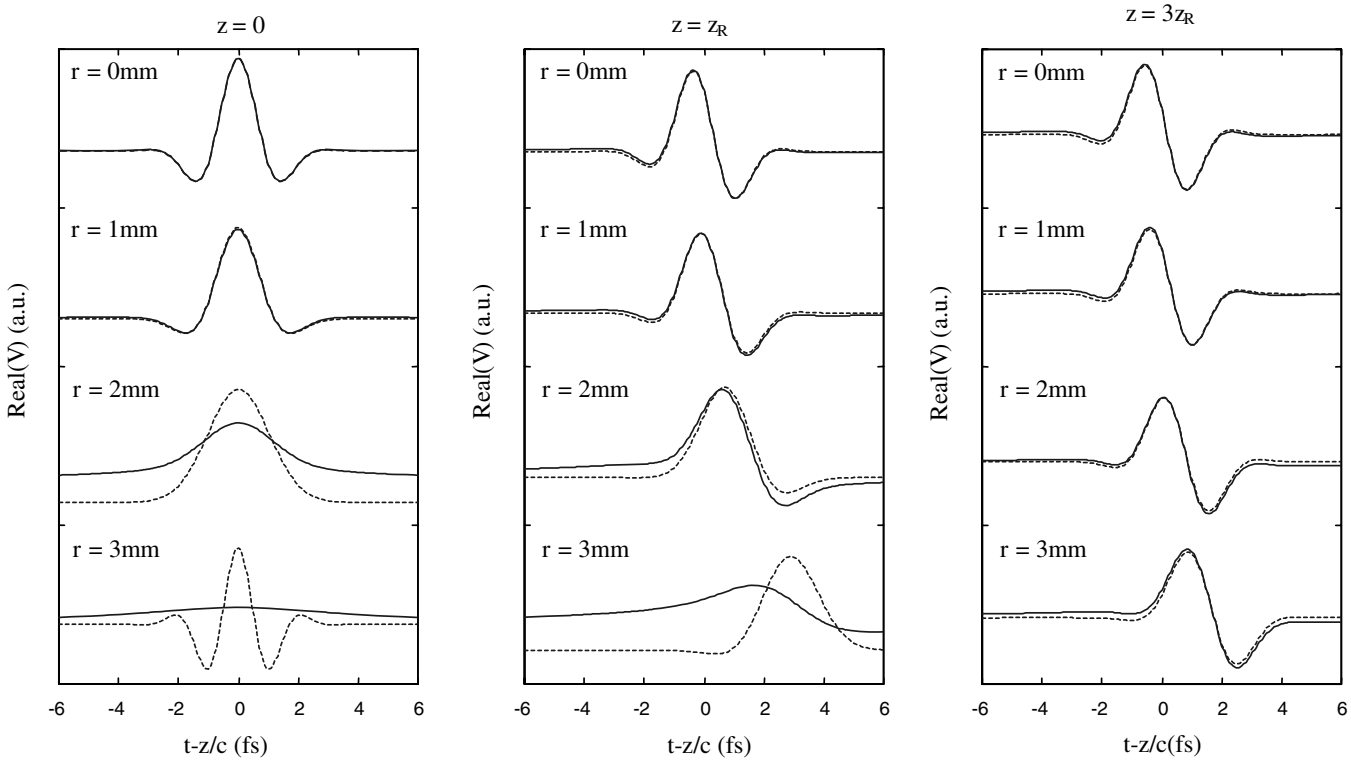

Fig. 4. Temporal waveforms of the PGB with $\gamma = 0.32$. The solid lines are real parts of V_{CAS}. The dashed lines are real parts of V_{CAE}.

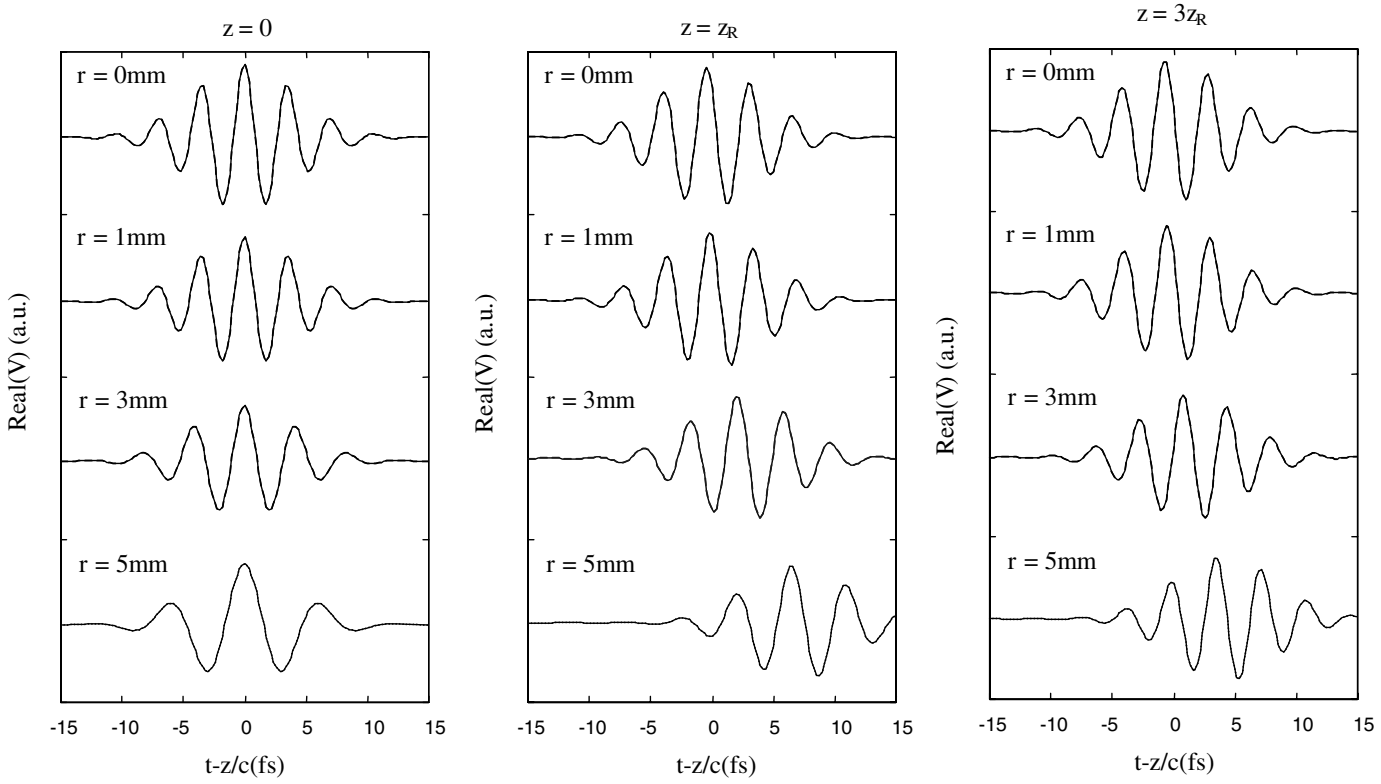

Fig. 5. Temporal waveforms of the PGB with $\gamma = 0.08$. The solid lines are real parts of V_{CAS}. The dashed lines are real parts of V_{CAE} (the dashed lines cannot be seen because the two lines coincide with each other).

$$V_{\mathrm{CAE}}(r,0,0)=\exp\left(-\frac{r^2}{w_0^2}+a_{\mathrm{g}}^2\frac{r^4\gamma^2}{w_0^4}\right). \tag{25}$$

From Eq. (25), it is found that the emergence of singularity of V_{CAE} is caused by the existence of a term $\exp\left(a_{\mathrm{g}}^2\frac{r^4\gamma^2}{w_0^4}\right)$, which results in the tendency of energy to infinite as r increases. At the same time, this term indicates that V_{CAE} also depends on bandwidth γ of the PGB. The term takes small value and singularity emerges far from z-axis in the case of narrowband, and vice versa. Eq. (22) at $z=0$ and $t=0$ can be written as

$$V_{\mathrm{CAS}}(r,0,0)=\exp\left(-\frac{r^2}{w_0^2}+a_{\mathrm{g}}^2\frac{r^4\gamma^2}{w_0^4}\right)\eta, \tag{26}$$

where

$$\eta=\frac{1}{2}\left\{1-\mathrm{erf}\left(-\frac{1}{2a_{\mathrm{g}}\gamma}+a_{\mathrm{g}}\gamma\frac{r^2}{w^2}\right)+\exp\left(2\frac{r^2}{w^2}\right)\times\left[1-\mathrm{erf}\left(\frac{1}{2a_{\mathrm{g}}\gamma}+a_{\mathrm{g}}\gamma\frac{r^2}{w^2}\right)\right]\right\}. \tag{27}$$

As compared with Eq. (25), the factor η is concluded in Eq. (26), which leads that Eq. (26) tends to zero as r increases. By using Eqs. (25) and (26), radial distributions of amplitude of the PGB with $\gamma=0.32$ and $\gamma=0.08$ at $z=0$ and $t=0$ is depicted in Fig. 6, from which it is seen that amplitude distribution of CAE solution makes a great deal of difference with that of CAS solution with broadband but few difference in the case of narrowband near z-axis. As can be seen, CAE solution with broadband is failed to describe the PGB (Fig. 6(a)), but in the case of narrowband the solution keeps Gaussian shape and singularity of it emerges far from z-axis (Fig. 6(b)), in which the singularity can be neglected.

It is noted that the PGB with $\gamma=0.08$ is not narrowband pulsed beam in the strict senses. In this paper, the reason that the PGB with $\gamma=0.08$ is included in narrowband pulsed beam is that $r_{\mathrm{s}}>10w_0$ is regarded as condition that the singularity can be neglected at the plane $z=0$ and there are few differences between CAE solution and CAS solution within the framework considered in the case of $\gamma=0.08$. Obviously, within the condition stated, CAE representation can be used for the PGB with $\gamma=0.08$ and CAS representation should be adopted for the PGB with $\gamma>0.08$, namely $\gamma=0.08$ can be regarded as a critical condition to determine what representation should be adopted.

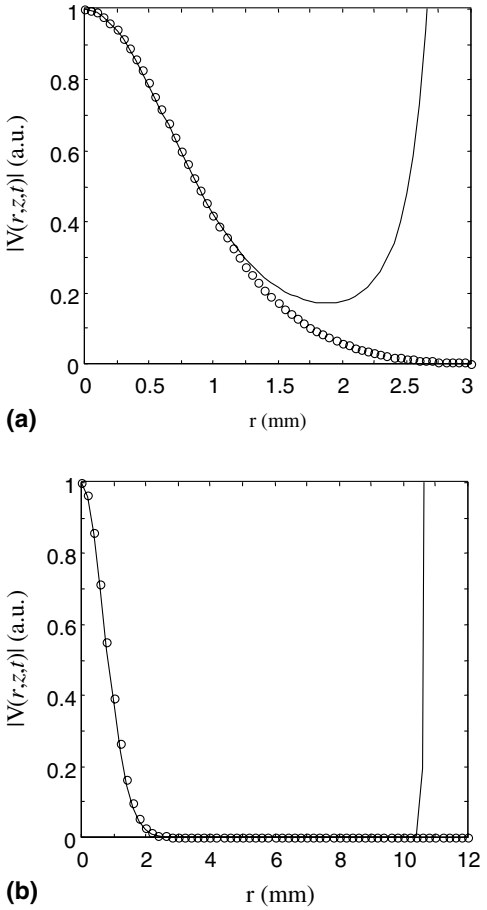

Fig. 6. Radial distributions of amplitude at $z=0$ and $t=0$ of the PGB with: (a) $\gamma=0.32$; (b) $\gamma=0.08$. The solid lines are that of CAE solution. The circle lines are that of CAS solution.

5. Conclusions

In this paper, CAE and CAS representations used to study propagation properties of the PGB are compared detailedly. Numerical calculations illustrate that it is CAS representation rather than CAE representation that should be used for the PGB with broadband ($\Delta\omega/\omega_0\sim1$). The reason for it is that singularity emerges near

z-axis for CAE solution, which is failed to describe the PGB. But for the PGB with narrowband ($\Delta\omega/\omega_0 \ll 1$), because singularity locates far from z-axis for CAE solution and field distributions near z-axis are the same as that of CAS solution, the SVEA can be performed and CAE representation is applicable. In addition, CAE solution with broadband is failed to show frequency shift, which is reported to be one of characters of the PGB, but CAS solution is able to show it both in the case of narrowband and in the case of broadband. Hence, it is necessary to choose approach appropriately in the study of PGB with different bandwidth. The results obtained in this paper demonstrate that, under certain conditions, CAE representation can be used if the bandwidth of PGB satisfies $\gamma = 0.08$. Other pulsed beams, such as Lorentz pulse and Hyperbolic Secant pulse, are also faced with the same problems mentioned in introduction. Further study for them seems to be necessary and the approach in our paper is applicable to them.

Acknowledgements

This work was supported by the Foundations of the State Key Laboratory of Laser Technology and the National Hi-Tech Project of China.

References

[1] I.P. Christov, Opt. Commun. 53 (1985) 364.
[2] Z.Y. Wang, Z.Q. Zhang, Z.Z. Xu, Q. Lin, IEEE J. Quantum Electron. 33 (1997) 566.
[3] Z.Y. Liu, D.Y. Fan, J. Mod. Opt. 45 (1998) 17.
[4] M.A. Porras, Phys. Rev. E 58 (1998) 1086.
[5] M.A. Porras, J. Opt. Soc. Am. B 16 (1999) 1468.
[6] M.A. Porras, R. Borghi, M. Santarsiero, Phys. Rev. E 62 (2000) 5729.
[7] M.A. Porras, Phys. Rev. E 65 (2002) 026606.
[8] X. Fu, H. Guo, W. Hu, S. Yu, Phys. Rev. E 65 (2002) 056611.
[9] D.Q. Lu, W. Hu, Y.Z. Zheng, Z.J. Yang, Opt. Commun. 228 (2003) 217.
[10] M. Born, E. Wolf, Principles of Optics, seventh ed., Cambridge University Press, Cambridge, 1999.
[11] A.E. Siegman, Lasers, University Science, Sausalito, 1986.